DR. Mahmoud Ali Attia

E-mail: Dmahmoud_75@yahoo.com

PROF. DR. Amr Mohamed Radwan:

E-mail: amrrad183@yahoo.com

E-mail:amrradwan590@gmail.com

Amal Hammad:

Civil Engineering Department, Faculty of Engineering, Helwan University, Egypt

E-mail: engamalhammad1989@gmail.com

DR. Ahmed Farag:

Email: AhmedAbdallah@oi.edu.eg

The behavior of underground conduits buried in soil

ABSTRACT

Many industries use pipelines for transporting various materials, including water, gas, oil, and sewage. A thorough study of the behavior of pipes and soil is essential in the design of buried pipes. The study goal is to forecast the performance of buried HDPE and fiberglass pipes at different thicknesses of sand backfill. A tank-shaped laboratory model of a trench and top static stress is built. PLAXIS-2D finite element software was employed to validate the experimental test values. A parametric study is performed to investigate the potential impacts of the ground loads, the loading area length, the pipeline's buried depth, and the pipeline's type and wall thickness on the model response. From the results, it can be concluded that pipes buried at shallower depths are subjected to significantly greater stresses and damage ratio. The physical and numerical modeling results agree with each other. It is also observed that if the parameters are well selected for physical and numerical analysis, it can be an easy and less time-consuming method for finding out strength and deformation behavior for analyzing and designing the buried pipes. Generally, the pipes with greater wall thickness and depth are safer within a reasonable range. Therefore, it can be concluded that this methodology can be used for the safe and economical design of buried pipes subjected to static loading conditions.

Keywords: Buried flexible pipe, pipe burial depth, Soil Box Test, and trench conditions

1. Introduction

The integrity and performance of buried pipe infrastructure play a significant role in modern society; providing the safe distribution of potable water, transportation of sewage, and connection of communication services, amongst other applications. For this purpose, a diverse range of buried pipes is deployed such as large-diameter concrete sewer pipes to small-diameter plastic freshwater pipes. Municipal water distribution and wastewater infrastructure systems are of national importance and the aspect of water leakage, coupled with water scarcity, has become a serious problem in many countries. Typically, utility pipes are located beneath the surface of road networks to simplify installation, distribution, and maintenance. Owing to the shallow burial depth of these critical infrastructure assets, they are highly vulnerable to a number of factors that may influence their performance and deterioration; for example, the impact of heavy surface traffic loading and changeable burial conditions. A realistic estimation of load distribution over the buried structures is necessary for proper analysis of pipes/conduits, culverts, and tunnel lining. Pipelines are often constructed in the areas of civil engineering, mining

engineering, agriculture, and some other areas. For the design of a pipeline, it is essential to know the load over it. Load distribution over the buried structures has been investigated scientifically during the past several decades. The method of investigation includes experimental, analytical, and numerical methods. For the safety aspect, the interaction between the pipe and surrounding soil is an important factor in expecting better performance. That is why many researchers have investigated the load distribution on the buried pipe in the past (Marston 1930; Valsangkar and Britto 1978, 1979; McVay and Pappadopoulos 1986; McVay et al. 1993; Arockiasamy et al. 2006; Talesnick et al. 2008; Chaallal et al. 2015a, b; Li 2016).

Chapman et al. (2007) investigated the deformation of polyvinyl chloride (PVC) pipes under static surcharge. The authors found that both the load transferred to a buried pipe and the pipe vertical deflection decrease with increasing degree of soil compaction because of improved arching effect. Tafreshi and Khalaj (2011) investigated the behaviors of a buried HDPE pipe at different embedment depths under both static and cyclic loads, finding that burial depth, the amplitude of surface pressure, and soil density affected pipe behaviors. Chaallal et al. (2015a) conducted field tests on buried pipes made from HDPE, PVC, and metal. The results indicate that the vertical pipe deflection decreases significantly when the soil cover depth increases from 0.5D to 1.0D, where D is the pipe diameter. Only an insignificant decrease in pipe deflection is observed when the cover depth further increases to 2.0D. This observation is consistent with that reported by Arockiasamy et al. (2006). Rakitin et al. (2016) experiments on concrete pipelines show that when the buried depth of the pipeline increases, the increase of the bending moment of the pipeline caused by the self-weight of the soil is much smaller than the decrease of the bending moment caused by the traffic load. Saboya et al. (2020) studied the deformation of the steel pipe buried in cohesionless soil under moving surface loads. Experiments showed that when the pipe was installed in a shallow depth, the cross-section of the pipe changed from a vertical ellipse to a horizontal ellipse under a moving surface load. Tian et al. (2019) studied the influence of buried depth on the impact force and acceleration of pipelines under impact load. The results showed that the maximum acceleration and impact force on the pipeline decreased with the increase of buried depth because the vibration wave attenuated rapidly with the increase of distance. Zhang et al. (2023b) investigated the effect of pipe installation and external load on buried steel pipe and concluded that when increasing the pipe wall thickness, the maximum bending moment increases while the maximum pipe stress decreases

during the soil compaction procedure. The increase in bending moment is due to the increased pipe rigidity. However, the pipe stress is inversely proportional to the square of the pipe wall thickness. Mohammed (2017) studied the circular tunnels under static and dynamic loads at different depths showing that the depth of the tunnel has a significant effect on the stability behavior. Kumar et al. (2017a) studied the deformation behavior of tunnels under different Loading Conditions and concluded that shallow tunnels are more vulnerable to damage as compared to deep tunnels. As the overburden depth of the tunnel increases, the effect of damage will decrease.

Cao et al. (2016) investigated the effects of cyclic traffic loading on the behaviors of a flexible pipe buried at a shallow depth in a full-scale plate load test, evaluating the permanent deformation of the pipe. They found that the buried pipe had minimal deflection under cyclic traffic loading, and as the stiffness of the buried pipe increased in the parametric study under numerical analysis, the road surface permanent deformation was magnified; similarly, the road surface deformation decreased as the pipe embedment depth increased. Chaallal et al. (2015b) numerically evaluated the deformation of buried HDPE pipes under static loading. The vertical pipe deflection and the pipe strain decrease with increasing soil cover depth and degree of soil compaction. Similar behavior was observed by Bryden et al. (2015) based on a numerical investigation of fiber-reinforced plastic pipes. Neya et al. (2017) numerically studied the impact of dynamic load on the response of a buried steel pipe assuming both soil and pipe are elastic materials. The pipe stress was found to decrease with the increasing cover depth, truck moving speed, and soil stiffness. Abdelfateh et al. (2021) presented a method for modeling the behavior of a pipeline based on the finite element analysis by using PLAXIS 3D software, which was aimed at the determination of the pipe bending moment, the displacement over its length, and the evaluation of the vertical stresses in the soil under the pipe. A parametric study was carried out to investigate the effect of the depth of the pipe burial and the soil cohesion. It was found that, unlike laboratory models, the numerical analysis could account for the internal pressure in the pipe and the depth of the pipe burial.

Therefore, in this research, a static loading test was performed after pipe installation at a cover depth of 0.15m. Then, a two-dimensional numerical model was generated and validated based on the experimental data. Thereafter, a series of parametric studies were performed to investigate the impact of factors including pipe type and wall thickness, loading area, and soil lift thickness. Finally, the main conclusions are

summarized based on the experimental and numerical results. The works presented in this paper provide some insights into the flexible pipe behavior under the effect of external static load. The behavior of the pipe was assessed by investigating its deformation and generated stresses above its crown.

2. Research Objectives

The main aim of this study is to investigate the behavior of buried HDPE and fiberglass flexible pipes in sand soil, which would provide a deeper understanding and enhance the knowledge of the system's performance. Furthermore, it would provide data to calibrate numerical models, which would simplify the investigation process under various conditions, including loading, soil properties, burial depth, and properties of buried utilities which would enable avoidance of system failure. Then investigate the following steps to design a sewage line safely

- First, the stresses caused by traffic and the intensity of traffic on the road must be known.
- The suitable buried depth for the pipeline is known.
- It is necessary to know the distribution of stress from the ground surface until it reaches the pipe beds.
- The amount of stress on the soil underneath the pipe bedding and the soil-bearing capability must be determined. In order to prevent the soil from collapsing under the pipe, it is important that the soil stress values do not exceed its bearing capability.
- Although the stress under the bedding of the pipe is safe, the pipe is still not considered safe unless the deflection is checked so that it does not exceed the permissible values.
- The stress values at the top of the pipe should not cause the pipe to deflect more than the allowed values (5%), in order to prevent damage to the pipe.

3. EXPERIMENTAL PROGRAM

To assess the performance of buried HDPE and fiberglass pipes, a series of fully instrumented large-scale laboratory tests were performed. Pipes were buried in sand beds. The system was subjected to incrementally increasing static loading, representing different vehicle loads or an increase due to additional applied loads.

3.1 Soil Box

The experiments were conducted in a rigid testing tank of 1000 mm in length, 210 mm in width, and 680 mm in height, which was designed and manufactured based on

recommendations of previous studies (Perkins and Edens, 2003; Arockiasamy et al., 2006; Tafreshi et al., 2012; Hussein et al., 2015; Hussein and Meguid, 2016; Peter et al., 2019; Elsheshney et al., 2020). In order to avoid the effect of boundary conditions, i.e. reaction interference, the tank length should be more than six times the pipe diameter, and therefore the tank length was selected to be 1000 mm. The tank width was taken to be the same as the pipe length As a result, choosing the width of the tank to be 0.21 m was not expected to cause an interference. The depth of the tank was chosen to be 0.68 m to allow installation of the pipe at three different burial depths. Consequently, a rigid testing tank, 1000 mm in length, 210 mm in width, and 680 mm in height was designed and manufactured. Steel of 12 mm thickness was used to construct the testing tan k. To avoid the effect of boundary conditions, the internal faces of the testing tank walls were painted with epoxy. Consequently, during testing, the friction generated between sand particles and the walls of the tank was minimized. The tank was centered under the loading frame, which was connected to a Hydraulic jack, forming the loading system, which was used to apply predetermined incrementally increasing static loading profiles. Steel rigid box stiffeners were used to maintain the rigidity of the walls of the testing tank.

3.2 Physical model

A strip footing was used in this study to transfer the load to the pipe soil system. A rectangular-shaped steel plate with 250 mm in length and 200 mm in width was used as a strip footing. The footing length was 10 mm shorter than the width of the tank, to avoid the potential frictional effect between the footing and the tank walls. The function of the footing in the research is to transfer the applied load to the system beneath it and convert it into pressure.

A calibrated load cell was installed between the loading shaft and the footing to obtain high-quality data. To capture the pressure on the pipe, an earth pressure cell was installed directly at the crown. This pressure cell would enable the provision of data for the pressure distribution as the test progressed. Furthermore, it is generally understood that the interaction of the pipe and the soil, rather than the pipe alone, governs the behavior of buried pipe. Therefore, it is useful to observe the behavior of the soil during the tests to assess the probability of soil-pipe deformation under various loading conditions therefore; Digital cameras and a photogrammetric system have been used to assess the coordinates of signalized targets on structural components during static load testing in order to study soil-pipe behavior. The calibration of the digital photogrammetry technique was done by comparison between divisions on the Perspex front and divisions obtained by digital photogrammetry.

3.3 Materials Used

In order to determine the required soil parameters, a soil-testing program was carried out. Routine soil tests were carried out to characterize the soil properties, namely, specific gravity, grain size analysis, direct shear test, and modified Proctor compaction test. The

mechanical grain size analysis according to ASTM D422-07 was performed on the backfill material. The physical and mechanical properties of the sand are summarized in Table 1. The grain size distribution curve of sand soil is shown in Figure 1. The pipe used in the study was made of HDPE (high-density polyethylene) and fiberglass with an external diameter of 150 mm and 4 and 6 mm wall thickness. They are recognized in applications for urban services including drainage and sewage systems. The length of the pipe is 1 cm less than the width of the tank to prevent binding against the end walls and boundary condition impacts.

Table 1: characteristic of the used sand

Index Property	Standards	Value
Specific gravity (Gs)	ASTM D-854	2.68
D10 (mm)	ASTM D 422	0.225
D30 (mm)	ASTM D 422	0.394
D60 (mm)	ASTM D 422	0.588
Coefficient of uniformity (C_u)	-	2.61
Coefficient of curvature (C_c)	-	1.17
Soil Classification according to (USCS)	ASTM D 422-07	SP
Friction angle	ASTM D 3080-03	Dense state: $\varphi = 36.5^0$
Friction angle	ASTM D 3080-03	Medium state: $\varphi = 34^0$

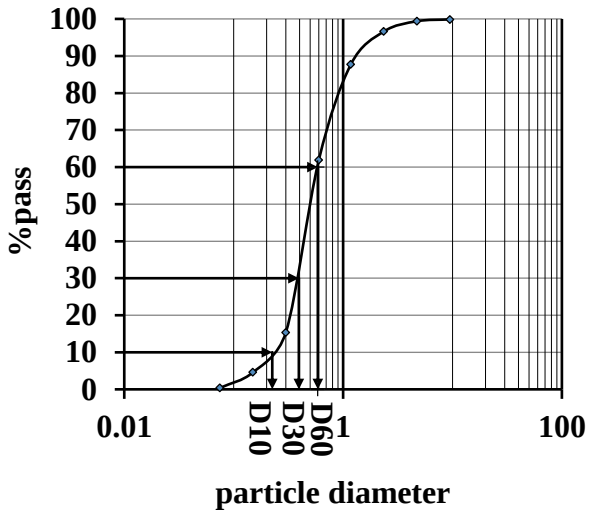

Figure 1: Grain size distribution curve of sand

3.4 Testing Procedure

The tank sample for each test was prepared separately by placing granular soil compacted to a maximum dry density of 85% at the bottom and lateral sides of the tank in a U shape. Before putting the trench material, the pipe should be in place while pressure cells are attached to the pipe in appropriate positions. Then, after placing the pipe, trench soil or sand material was to be placed and compacted in the trench area. The trench width is 55 cm and this width was chosen according to AASHTO recommendation in which trench width should not be less than the greater of 1.5 times the pipe outside diameter plus 300 mm or the pipe outside diameter plus 400 mm. The trench height varies depending on the embedment depth of the buried pipe (1D, 1.67D, and 2.33D) and changes between 300 to 500 mm which is the sum of burial depth plus pipe diameter. Soil compaction was performed with an appropriate hammer to simulate compaction in the field to reach 95% maximum dry density. The height of the trench was divided into equal strips so that the soil in each layer (i.e. 6 cm thickness) was compacted separately. The soil weight required in each layer was calculated from considerations of soil unit weight and chamber volume. At the end, the surface of the soil was leveled. In the last step, the loading cell and the loading plate were centered in the tank as shown in Figure 2. To measure the short-term behavior of the pipe-soil system, experiments were carried out using uniform surface pressure increments ranging from 0 kN/m^2 to 200 kN/m^2. A digital camera mounted on a tripod was placed in front of the viewing window and Photographs obtained throughout the testing allowed for measurements of pipe and foundation soil displacements.

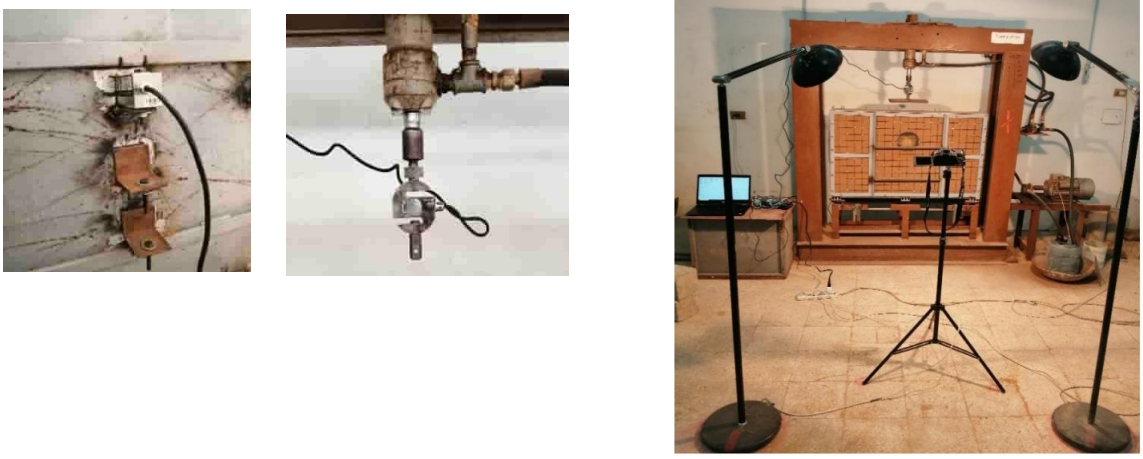

(a) (b)

Figure 2: (a) load cells, (b) Experimental setup

4. NUMERICAL MODELLING

4.1 The software presentation

PLAXIS is a powerful and user-friendly finite element program used for geotechnical engineering and design all over the world. It offers advanced constitutive models for simulating nonlinear, time-dependent, and anisotropic soil and rock behavior. PLAXIS 2D, a program designed for two-dimensional analysis in a variety of applications ranging from excavations, embankments, and foundations to tunneling mining and reservoir geomechanics, was employed specifically for this project.

4.2 Two-dimensional modeling of the buried pipe tests

The study goal is to estimate the deflections and loads of a buried flexible pipe while taking into account the stages of construction and the pipe-soil interaction. In the analyses, uniform surface loads and earth loading are assumed uniform over the pipe length. The pipe will be subjected to loads that act only in the x and y directions for this type of analysis, and the trench-pipe system (pipe and backfill material) has a cross-sectional area that is constant for an undetermined length in the z-direction. Due to the nature of the problem, it is possible to assume that the state of strain is normal to the x-y plane ε_z and the shear strains τ_{xz} and τ_{yz} are both zero. This strain state is known as the plane strain condition because it reduces the calculation to a two-dimensional analysis (Logan 2012). Therefore, in these analyses; the plane strain model is applied.

A numerical Model based on the cross-sections of the experimental test is shown in Figure 3. The width and height of the numerical model were 1.00 m and 0.68 m, respectively. A 0.55 m wide by 0.35 m deep trench was excavated at the center of the numerical model. The boundary conditions were assigned as follows: the bottom of the soil was fixed at all degrees of freedom, while only horizontal deformation was restricted at the sides. With a diameter of 0.15 m, the pipe was created using the tunnel designer tool. To simulate the tangential behavior at the pipe-soil interface, a strength reduction factor R_{inter} of 0.7 was set at the soil-pipe interface (Zhou et al., 2017). To represent the backfill, fifteen nodding plane strain triangular elements were employed, and the soil is expected to follow the hardening soil model. The fine mesh was chosen in this investigation to improve the accuracy of the result, mesh was refined within the trench zone and near the pipe, where the majority of the stress change and deformation occurs. The soil elements inside the pipe were excavated to be void after the pipe was installed. This study does not consider groundwater. A strip surface pressure ranging from 0 kN/m^2 to 200 kN/m^2 was applied on the ground surface on 0.25 m width, along the length of the pipe. The pipe embedment ratio (H/D) varied between 1, 1.67, and 2.33, where H is the distance between the pipe crowns and the ground surface, and D is the pipe exterior diameter.

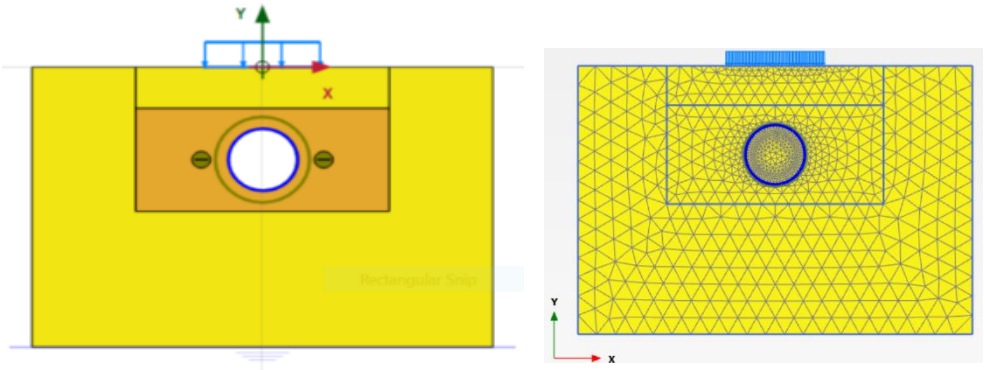

(a) **(b)**

Figure 3: (a) Two-dimensional finite element model for fiberglass and HDPE pipes, (b) Generated mesh for the model

4.3 Soil Constitutive Model

To simulate the behavior of sandy soil, it was decided to use the Hardening Soil Model (HSM) because it is well adapted for granular soil under a monotonic and limited unloading stress path. In fact, by comparing it to other models, linear elastic and perfectly plastic models, which assume a Mohr-Coulomb (MC) criterion, it was possible to notice that the MC model has some inherent limitations such as linearity (constant E, v), unlimited dilation, isotropy, and perfect plasticity. In conclusion, the HSM model is more appropriate since it still includes the theory of plasticity and soil dilatancy, as does the MC model, but it introduces a yield cap and the elastic modulus is stress-dependent. The fundamental difference with the HSM is that the elastic domain is not fixed, but it does change in fact, it can expand based on the volumetric and deviator plastic strains and it has two unique yielding mechanisms: one in shear and one in compression. In odometer loading and isotropic loading, compression hardening is utilized to describe irreversible plastic strain caused by primary compression (Schanz et al., 1999). The elastic perfectly plastic model has different characteristics from the other versions, which is another difference between them. The Mohr-Coulomb model makes use of the following parameters: friction angle, dilatancy angle, cohesiveness c, Poisson's ratio v, and stiffness E. However, In the case of HSM, three stiffness parameters rather than one are examined. Figure 3 shows a two-dimensional finite element model for fiberglass and HDPE pipes at embedment ratio

(H/D) =1. Table 2 and 3 summarizes the pipe's physical properties.

Table 2: Input parameters for HDPE pipe

Parameters	
Normal stiffness, EA (kN/m)	4860
Flexural Rigidity, EI (kNm^2 /m)	0.01458
Equivalent thickness, d_{eq}, (m)	0.006
Weight, W (kN/m^3)	0
Poisson's ratio, v	0.43

Table 3: Input parameters for fiberglass pipe

Parameters	
Normal stiffness, EA (kN/m)	66000
Flexural Rigidity, EI (kNm^2	0.198
Equivalent thickness, deq, (m)	0.006
Weight, W (kN/m^2)	0
Poisson's ratio, v	0.29

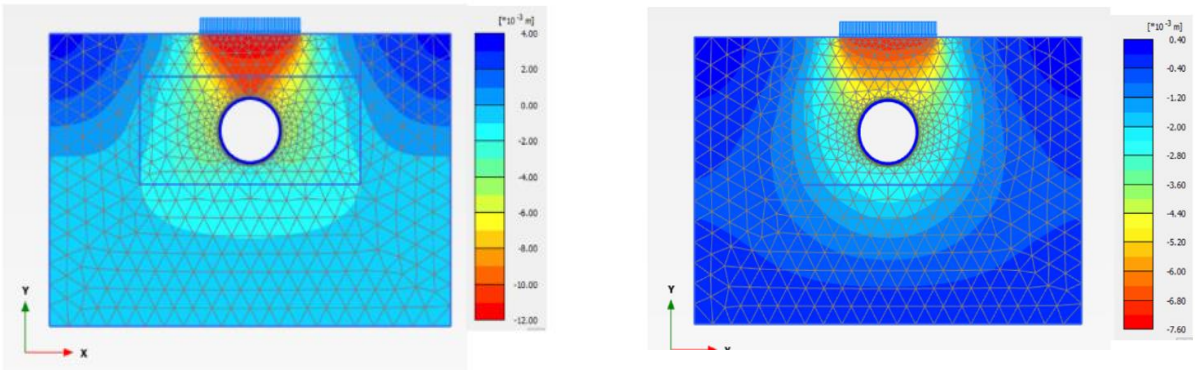

HDPE PIPE **FIBERGLASS PIPE**

(a)

HDPE PIPE **FIBERGLASS PIPE**

(b)

Figure 3: Two-dimensional finite element model results for fiberglass and HDPE pipes (a) Total displacements, and (b) Total normal stress

5. RESULTS AND DISCUSSION

Due to paper length limitation, just a brief overview of experimental results and numerical modeling will be presented.

5.1 Experimental work results

5.1.1 Effect of buried depth

Applying an experimental study, the effect of the embedment ratio against surcharge stress is studied. Under various surface stresses, the vertical crown deflection of HDPE and fiberglass pipes with varying wall thicknesses was measured. Figures 4 to 7 show the vertical and horizontal deflections of pipes for different sand soil embedment ratios (H/D) under different surface stresses. The findings demonstrate that the pipe behavior is mostly influenced by the magnitude of the surcharge surface stress where the crown deflection of the embedded pipe increases linearly as the surcharge stress in the sand increases. The findings also provide an explanation for why pipe crown deflections decrease as embedding ratios increase. It has been noted that decreasing the backfill causes the pipe crown deflection to increase for the same surface stress where small backfill results in direct stress transmission to the pipe. According to Bildik et al. (2012), pipe displacements increase linearly as surcharge stress rises, and the pipe is better protected by the backfill cover. Raj Kumar and Ilamparuthi (2008) concluded that as cover height is increased, the pipe is better protected and the pipe-soil system becomes more rigid.

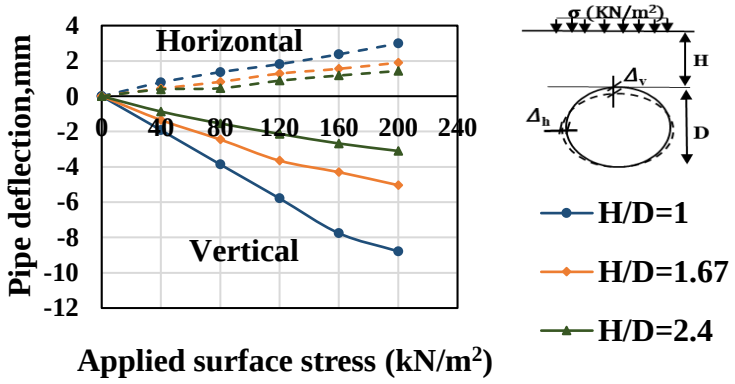

Figure 4: Influence of embedment ratio on deflections of 150 mm diameter HDPE pipe with thickness T= 6mm.

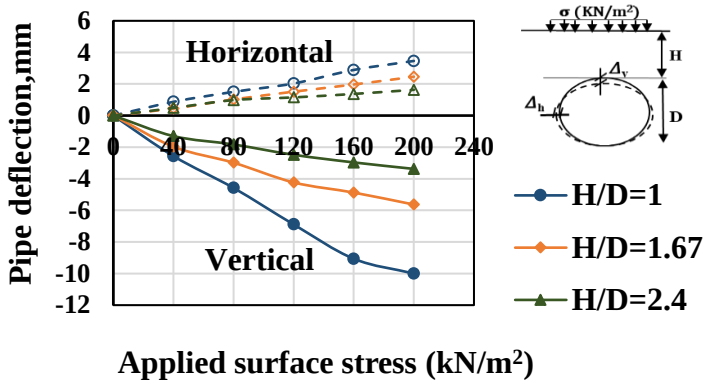

Figure 5: Influence of embedment ratio on deflections of 150 mm diameter HDPE pipe with thickness T= 4mm.

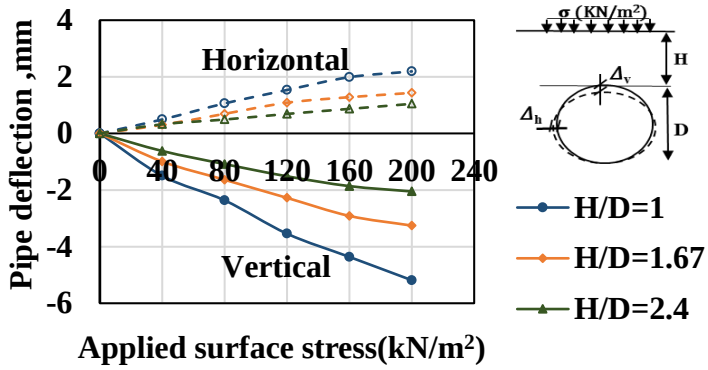

Figure 6: Influence of embedment ratio on deflections of 150 mm diameter fiberglass pipe with thickness T= 6mm.

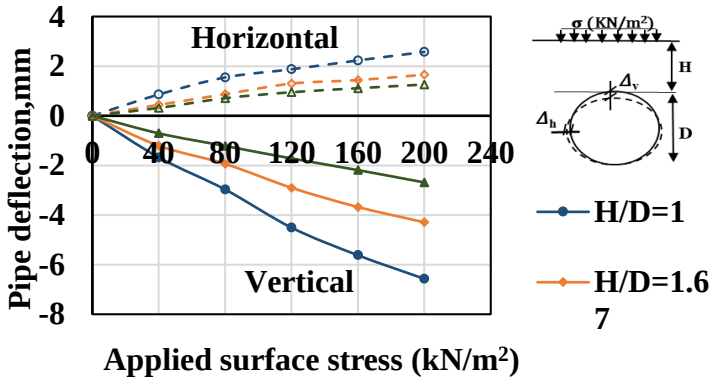

Figure 7: Influence of embedment ratio on deflections of 150 mm

5.2 Effect of pipe thickness

In order to understand how the thickness of the pipe section affected the pipe deflection and stress, the wall thickness was changed between 4 and 6 mm. For example under surface pressure of 200 kN/m^2 figures 8 and 9 show that as the pipe wall thickness decreased from 6mm to 4mm the pipe deflection increased for both types of pipe since the pipe is more flexible (easier to deform) . The behavior was the same at any applied stress.

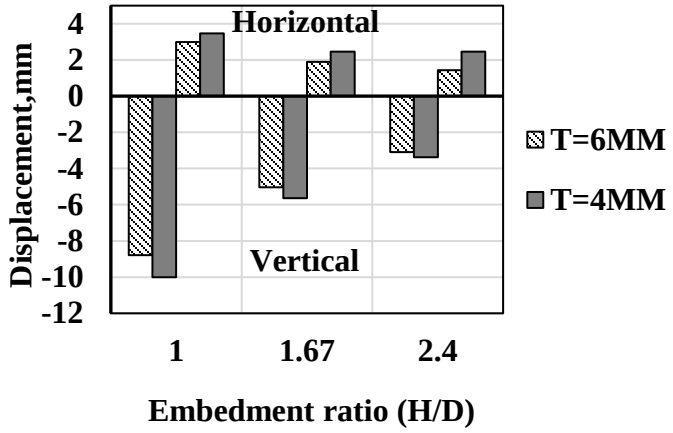

Figure 8: Comparison between diametric changes for different HDPE pipe wall thickness with embedment ratio, H/D at σ =200kN/m^2.

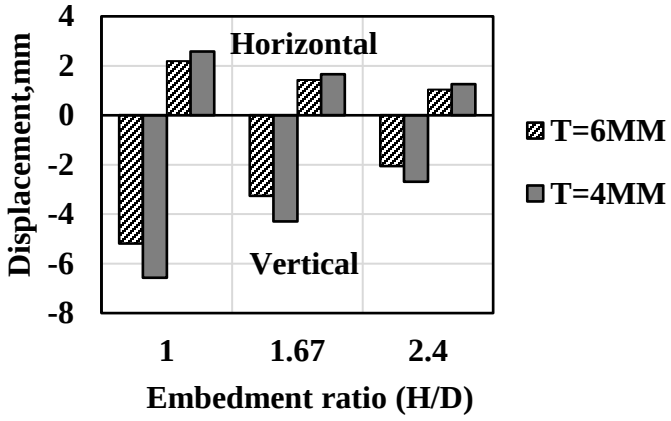

Figure 9: Comparison between diametric changes for different fiberglass pipe wall thickness with embedment ratio, H/D at σ =200kN/m^2.

Measured vertical stress at the pipe crown decreases with an increase in the embedment ratio. Figures 10, 11, 12, and 13 show a relationship between measured crown stress and applied surface stress curves for different embedment ratios H/D. As shown, increasing pipe burial depth was found to be highly effective in protecting buried pipes, as the selection of a greater burial depth facilitates the reduction in pipe stress and could aid with the longevity of the pipe lifespan.

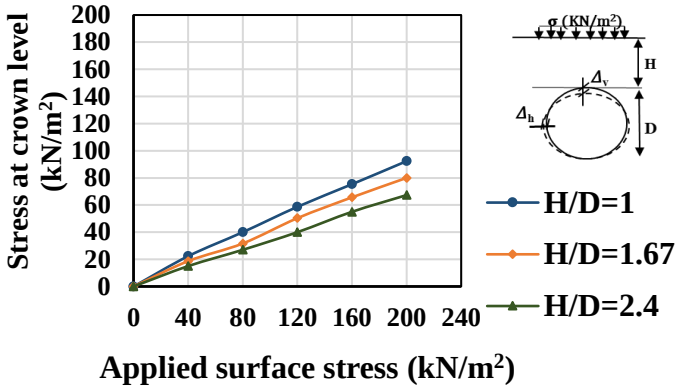

Figure 10: Influence of embedment ratio on stress at crown level for 150 mm diameter HDPE pipe with thickness T=6mm.

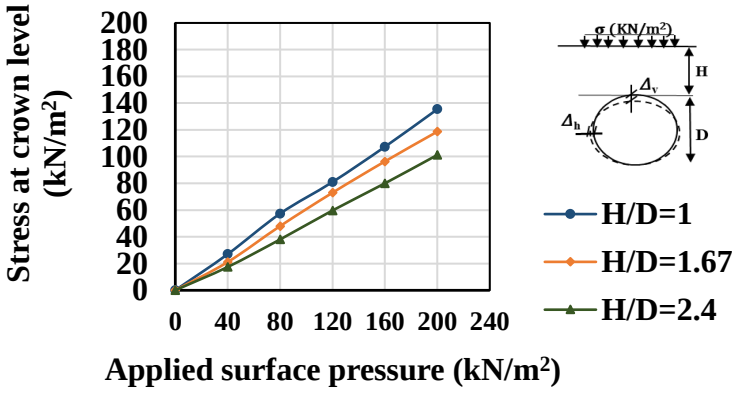

Figure 11: Influence of embedment ratio on stress at crown level for 150 mm diameter HDPE pipe with thickness T=4mm.

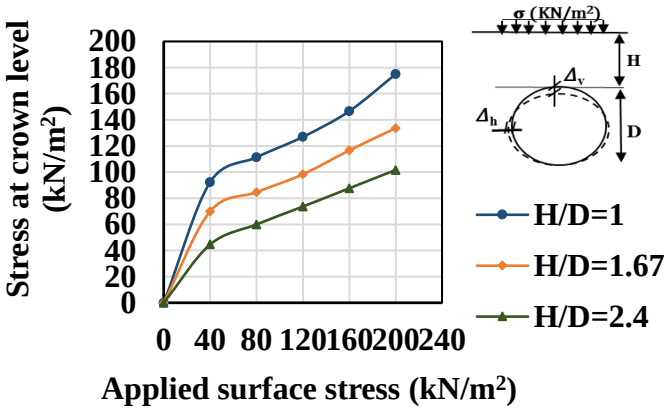

Figure 12: Influence of embedment ratio on stress at crown level for 150 mm diameter fiberglass pipe with thickness T=6mm.

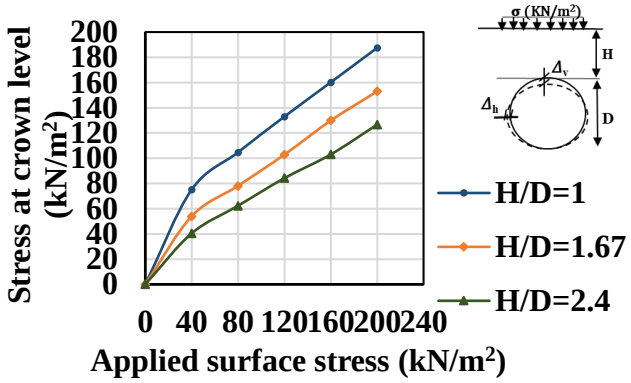

Figure 13: Influence of embedment ratio on stress at crown level for 150 mm diameter fiberglass pipe with thickness T=4mm.

5.3 Pipe Material (HDPE–Fiberglass) Effects

HDPE and fiberglass pipes were taken into account to examine the effects of pipe material on stress in thermoplastic pipes. It was determined that the stresses affecting the fiberglass pipe were higher than the HDPE pipe. The fiberglass pipe being stiffer than the HDPE pipe attracts more load compared to the HDPE pipe. Figure 14 shows a comparison between pipe crown stress for fiberglass and HDPE pipe with embedment ratio, H/D =1, and pipe wall thickness of 6 mm. However, it is important to note that the load-bearing capacity of the HDPE pipe-soil system was found higher than fiberglass pipe-soil system. The larger deflection of the HDPE pipe implies a larger increase in the horizontal diameter, which develops the lateral soil support and hence increases the load-carrying capacity of the ring. The behavior was the same at any embedment ratio and wall thickness. Similar results were obtained in the study by Kou et al. (2019) in which HDPE and PVC pipes were examined.

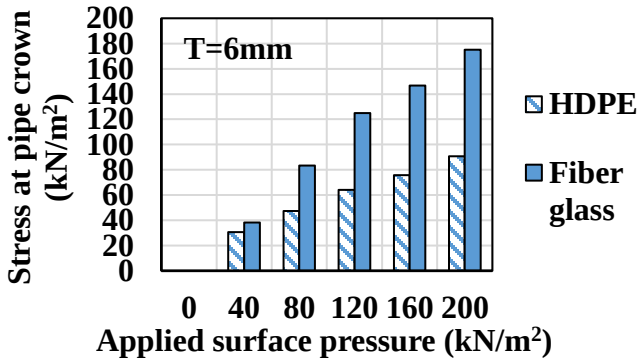

Figure 14: Comparison between pipe crown stress for fiberglass and HDPE Pipe with embedment ratio, H/D =1.

6. Comparison between experimental results and finite element analysis

This section compares the results from numerical simulations and experimental tests and discusses the effects of burial depth and surface pressure on pipe deflection and stress variation.

Figure 15 shows the impact of change in burial depth and surface pressure on stress transmitted to the pipe crown obtained through experimental and numerical analysis. As illustrated, results from the two methods follow the same pattern and increasing burial depth leads to decreased pressure on the pipe crown. In addition, increasing surface pressure increases stress on the pipe as expected. The gap between the two graphs for different surface pressures is lower for deeper burial depths means the impact of surface pressure is more significant for shallower pipes compared to deeper pipes.

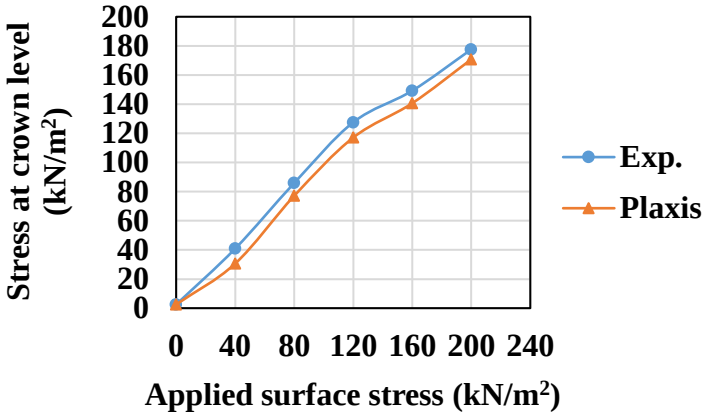

(a) H/D=1

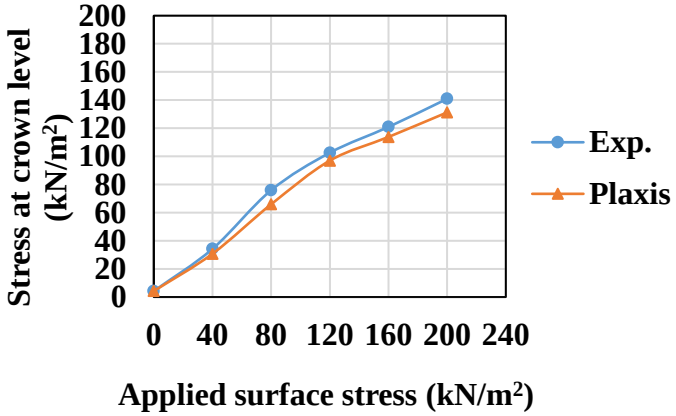

(b) H/D=1.67

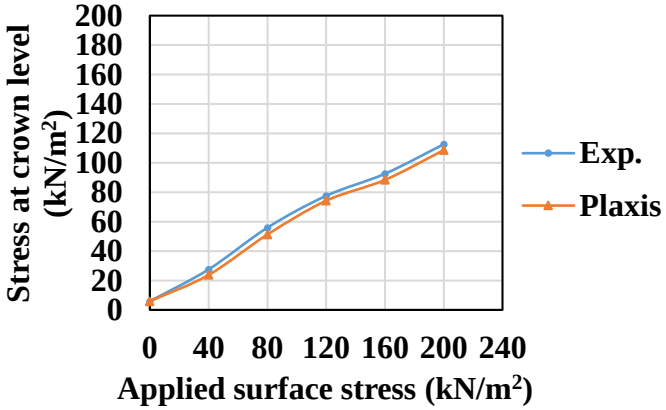

(c) H/D=2.4

Figure 15: Comparison between experimental and numerical stress measurements of fiberglass pipe of 150 mm diameter, and wall thickness of 6mm, buried at different embedment levels.

Deflection values of fiberglass pipe of external diameter of 150 mm and wall thickness of 6 mm buried at various depths of embedment levels (1D, 1.67D, and 2.33D) determined from the experimental studies and Finite Element Analysis using PLAXIS software both in the horizontal and vertical direction are shown in figure16. It is observed from the figure that the deflection of pipe is found to be higher along the direction of loading which will be almost double the times that the horizontal direction since the self-wt. of the cohesionless soil as well as the external incremental loading is applied over the crown of the pipe. The deflection is minimized by bedding the pipe at a greater depth hence; it is considered that the depth of the burial parameter plays a vital role in the reduction of vertical deflection of the pipe.

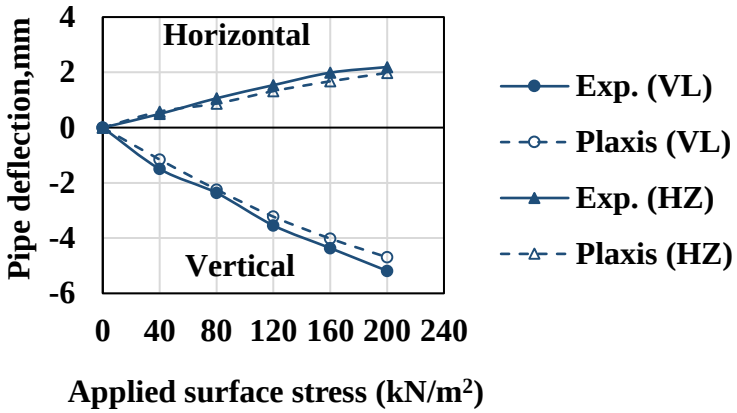

(a) H/D=1

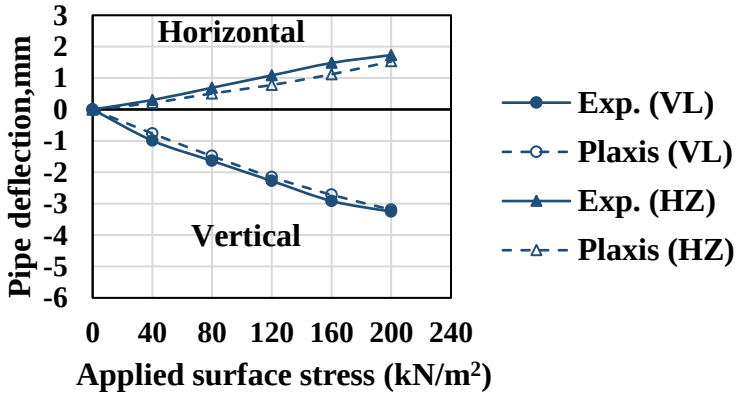

(b) H/D=1.67

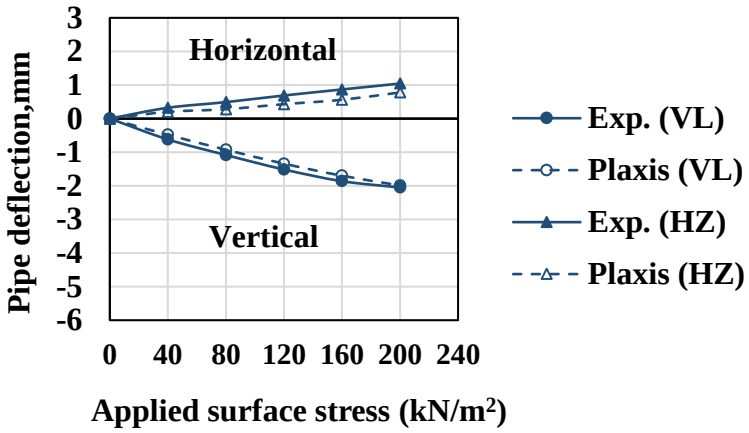

(c) H/D=2.4

Figure 16: Comparison between experimental and numerical deflection measurements of fiberglass pipe of 150 mm diameter buried at different embedment levels.

7. Formulation of a Stress Prediction Equation

For the development of the pipe stress prediction equation in the current study, the following variables are considered: traffic load (W), soil modulus (E_s), soil density (γ) , footing width (B), pipe diameter (D), pipe wall thickness (t), pipe modulus (E_p), and burial depth (h).

The functional relationship between maximum pipe stress and variable is as follows:

$\sigma_{max} = f\ (D, T, W_{vertical}, E_P, E_s, h, B)$.

In order to find the most effective stress prediction model, the various forms of functional relationships were thoroughly investigated.

$$X_1 = \frac{W * B}{t}, X_2 = \frac{W * D}{h}, X_3 = \frac{E_p * t}{E_S * h}, X_4 = \frac{W * h}{t}$$

$$\boldsymbol{\sigma}_{Max} = \alpha_1 X_1 + \alpha_2 X_2 + \alpha_3 X_3 + \alpha_4 X_4 \qquad (1)$$

The regression coefficients are shown in Table 4. The following units are used for the input variable in Eq. (1). The units of measurement for W, E_p, and E_s are kPa; t, B, h, and D are m; and the output stress is kPa.

Table 4: The regression coefficient values

Parameter	value
α_1	0.015
α_2	-0.1
α_3	6
α_4	$-4.1*10^{-3}$

7.1 The effect of applied surface stress on the stress at the pipe crown and in the bedding soil beneath the pipe.

The stress at the pipe was reduced with an increase in soil height over the pipe, according to the test findings; the main factor causing the decrease in pipe stress was the reduction of the stress intensity at the pipe crown with increasing depths because of the spread of stress within the soil .Therefore, it is considered that a depth of cover of 0.25 m and 0.35m (where the scale used in this study is 1:6) could be sufficient if the pipe was perfectly installed and no bedding settlement occurred over time. The stress value on the soil below the pipe bedding can be determined by extending the measured stress curve at the top of the pipe, as shown in Figure 17. The bearing capacity of the sandy soil beneath the pipe bedding was also determined to be 1.48 kg/cm^2, which is greater than the pressure that is being applied to it as shown in figure 18. This indicates that the pipe bedding soil can withstand stress without collapsing. Both bousinesq and the 2:1 distribution method were used to calculate the vertical stress at the pipe imposed by the static footing load. Figure 17 compares between the estimated pressures by two methods and the measured pressures on the pipe. The estimated pressures and the measured vertical pressures disagree. The measured stress on top of the pipe is significantly higher than the estimated stress; therefore, there is a major variance between the curves. As a result, the stress measured on the pipe crown does not distribute stress according to the Bousinesq and 2:1 approaches. However, there was great agreement between the new equation and the measured values of stress.

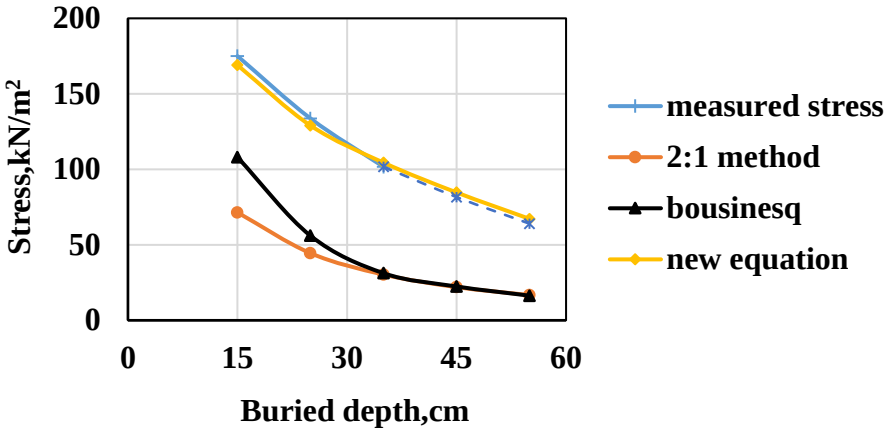

Figure 17: Measured versus calculated pressures above the fiberglass pipe under static loading

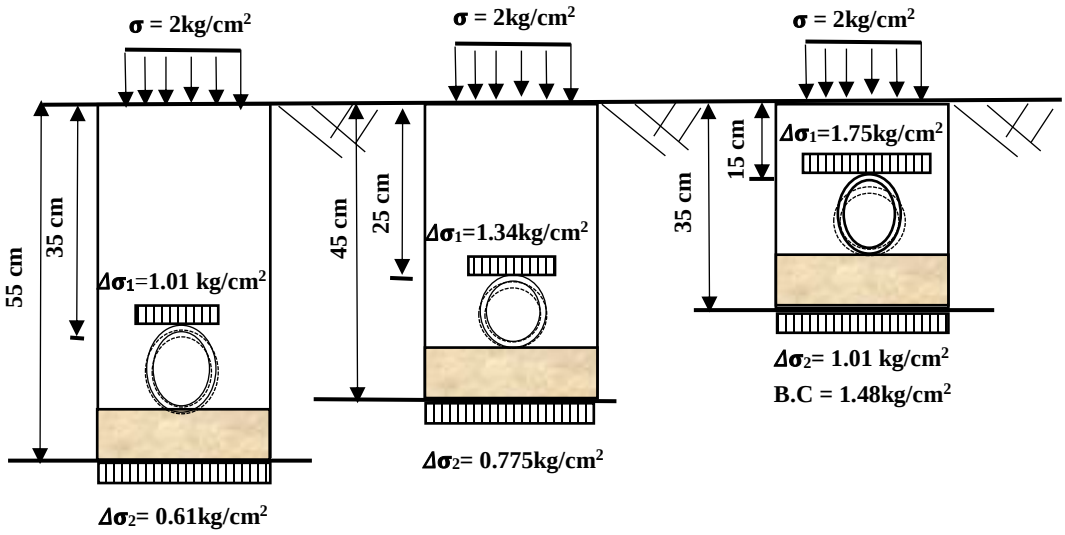

Figure 18: Measured stress at pipe crown and under pipe bedding

Where:

$\Delta\sigma_1$: the measured stress at the pipe crown.
$\Delta\sigma_2$: the measured stress under pipe bedding.
B.C: bearing capacity for the soil under pipe bedding.

7.2 Effect of measured stress at pipe crown on damage ratio

Three different cover depths were considered for this study. As illustrated in Figures 19 and 20, the embedment ratio (H/D) has an influence on the damage ratio, which is the ratio of the vertical pipe deflection percentage to the 5% deflection ratio. The results demonstrated that the expected vertical pipe deflection and damage ratio decreased with pipe buried depth. The principal damage ratios were found to be less than 1, which is consistent with the results of the laboratory static loading test and numerical analysis. This indicates that the expected vertical deformation of the pipe is less than the 5% maximum. Except for HDPE pipe with both thicknesses of 4 mm and 6 mm, and an H/D ratio of one where the damage ratio exceeds the maximum. Because fiberglass has a higher material rigidity than HDPE, it has a significantly lower predicted damage ratio when used. Kumar et al. (2017a) concluded that shallow tunnels are more vulnerable to damage as compared to deep tunnels. As the overburden depth of the tunnel increases, the effect of damage will decrease. Qian et al. (2021) also conclude that with an increase in the wall thickness and depth of the tunnel, there is a decrease in the extent of damage in the utility tunnels.

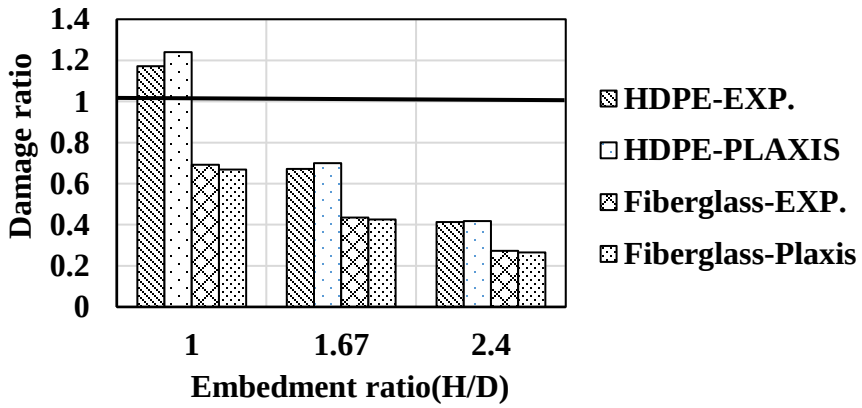

Figure 19: Effect of embedment depth on damage ratio for HDPE and fiberglass pipes

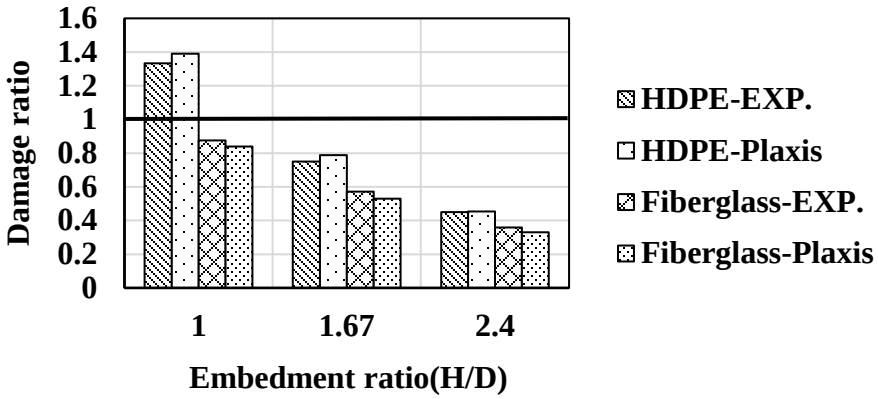

Figure 20: Effect of embedment depth on damage ratio for HDPE and fiberglass pipes

8. Conclusions

Two types of pipe with two different wall thicknesses were tested at three different burial depths under static surface loading. Diameter change and pipe crown stress were measured to understand the pipes' performance under the applied loads. Based on laboratory static load tests and finite-element analysis, the following conclusions are drawn.

- HDPE pipe deflects more than fiberglass pipe because it has less modulus of elasticity.
- The bearing capacity of the HDPE pipe–soil system is higher than of the fiberglass pipe-soil system, because of lateral soil support development in the case of HDPE pipe due to larger horizontal deflection.
- It is observed that the pipe has a higher resistance to load distribution when the soil is higher above the pipe.
- The results recommend that deflection is minimized by bedding the pipe at a greater depth since the load is distributed uniformly throughout the burial depth and hence minimum strain is experienced around the circumference of the pipe. Hence, it is considered that the depth of the burial parameter plays a vital role in the reduction of vertical deflection of the pipe.
- In addition, increasing surface pressure had a significant impact on increasing pipe deflection, soil surface settlement, and pressure on the pipe as expected.
- Good agreement between numerical and experimental test results was observed for both test series.

- Compared with the experimental work and FEM results, it has been found that the proposed stress formula is consistent with the measured results and numerical simulation of the pipeline stress.
- Despite the fact that the stress under pipe bedding is safe according to the soil's bearing capacity, the resulting deflection in the pipe must be less than the permissible values, otherwise, the stress affecting the soil must be reduced.
- Many parameters can affect the buried pipe's behavior such as pipe type, thickness, surface pressure, loading area, and buried depth, therefore a reasonable selection of these parameters can effectively reduce the maximum stress, strain, and ovality of the pipeline. In general, within a reasonable range, the pipes with greater wall thickness and depth are safer.

The magnitude of the deflection and the stress depends not only on the pipe's properties but also on the properties of the backfill soil. The magnitude of deflection and stress must be kept safely within the thermoplastic pipe's performance limits. Excessive deflection may cause a loss of stability, while excessive compressive stress may cause wall crushing or ring buckling. The key to solving the problem is to predict the stress and the deformation of the pipelines precisely before construction. In addition, to evaluate the impact degree of the construction on pipelines by considering various factors comprehensively such as the function, the material, the size of the pipeline, and so on.

9. Limitations and recommendations for future study

- It must be noted that in this research, two types of pipe material with one diameter were installed in one type of silica sand. Hence, the research outcomes are limited to these conditions. In the case of changing any of these variables, different outcomes could be obtained.
- To provide a further understanding of the behavior of buried pipes in response to external cyclic loading, this research could be extended in the cyclic phase.
- The current study in the experimental section was in the laboratory only and a full-scale field verification is still needed.

Reference

1. Abdelfateh, K. – Mohamed, B. – Fattah, M. Y. (2021) Numerical Modeling of the Pipeline Uplift Mechanism in Clay, Archives of Hydro–Engineering and Environmental Mechanics, Vol. 68 (2021), No. 2, pp. 119–135, DOI: 10.2478/heem–2021–0007.
2. Arockiasamy, M., Chaallal, O., & Limpeteeprakarn, T. (2006). Full-Scale Field Tests on Flexible Pipes under Live Load Application. Journal of Performance of Constructed Facilities, 20(1), 21–27.

3. ASTM D422–07: Materials Standard Test Method for Practical– Size Analysis of Soils, American Society for Testing and Materials, Annual Book of ASTM Standards.
4. ASTM, D3080 (2003) Standard Test Method for Direct Shear Test of Soils under Consolidated Drained Conditions, Soil and Rock (I), Vol. 04.08.
5. ASTM, D854 (2003) Standard Test Method for Specific Gravity of Soil Solids by Water Pycnometer, Soil and Rock (I), Vol. 04.08.
6. Bildik S., Laman M., and Suleiman M.T. (2012), " Parametric studies of buried pipes using finite element analysis", Proceeding of 3rd International.
7. Bryden, P., El Naggar, H., & Valsangkar, A. (2015). Soil-Structure Interaction of Very Flexible Pipes: Centrifuge and Numerical Investigations. International Journal of Geomechanics, 15(6), 1–11.
8. Cao Z, Han J, Xu C, Khatri DK, Corey R, and Cai Y 2016 Road surface permanent deformations with a shallowly buried steel-reinforced high-density polyethylene pipe under cyclic loading Geotextiles and Geomembranes 44(1):28-38.
9. Chaallal, O., Arockiasamy, M., & Godat, A. (2015a). Field Test Performance of Buried Flexible Pipes under Live Truck Loads. Journal of Performance of Constructed Facilities, 29(5), 1–10.
10. Chaallal, O., Arockiasamy, M., & Godat, A. (2015b). Numerical Finite-Element Investigation of the Parameters Influencing the Behavior of Flexible Pipes for Culverts and Storm Sewers under Truck Load. Journal of Pipeline Systems Engineering and Practice, 6(2), 1–13.
11. Chapman, D. N., Fleming, P. R., Rogers, C., & Talby, R. (2007). The Response of Flexible Pipes Buried in Sand to Static Surface Stress. Geomechanics and Geoengineering, 2(1), 17–28.
12. Elshesheny A, et al. In: Numerical behavior of buried flexible pipes in geogridreinforced soil under cyclic loading, vol. 122; 2020, 103493.
13. Hussein, M. & Meguid, M. 2016. A three-dimensional finite element approach for modeling biaxial geogrid with application to geogrid-reinforced soils. Geotextiles and Geo membranes, 44, 295-307. 26.
14. Hussein, M. G., Meguid, M. A., Whalen, J. & Eng., P. 2015. On the numerical modeling of buried structures with compressible inclusion. GeoQuebec, September, Quebec City.
15. Kou, Y.; Shukla, S.K. Analytical Investigation of Load over Pipe Covered with Geosynthetic-Reinforced Sandy Soil. Int. J. Geosynth. Ground Eng. 2019, 5, 5.
16. Kumar P, Shrivastava AK (2017a) Damage Detection in Shallow Tunnels Using 3D Numerical Modelling. In: International Conference on Advancements and Innovations in Civil Engineering 177–181.
17. Li Ch (2016) Developing an analytical method to study vertical stress due to soil arching during tunnel construction. J Geotech Geol Eng No 34:1247–1255.

18. Logan, D. 2012. A first course in finite element analysis. Stamford, CT: Global Engineering.
19. Marston A (1930) The theory of external loads on closed conduits in the light of the latest experiments. Bulletin 96, Iowa Engineering Experiment Station, Iowa State College, Ames, IA, USA.
20. McVay MC, Pappadopoulos P (1986) Long-term behaviour of buried large-span culverts. J Geotech Eng 112(4):424–442.
21. McVay MC, Pappadopoulos P Bloodmquist D (1993) ‘‘Longterm behavior of buried large-span culverts in cohesive soil.’’ Transportation Research Record 1414, Transportation Research Board, Washington, DC, pp 40–46.
22. Mohammed J (2017) Numerical Modelling for circle tunnel under static and dynamic loads for diferent depth. Research Journal of Mining 1(1):1–11
23. Neya, B. N., Ardeshir, M. A., Delavar, A. A., & Bakhsh, M. Z. R. (2017). Three-Dimensional Analysis of Buried Steel Pipes under Moving Loads. Open Journal of Geology, 7(01), 1–11.
24. Perkins, S. & Edens, M. 2003. Finite element modeling of a geosynthetic pullout test. Geotechnical & Geological Engineering, 21, 357-375.
25. Peter JM, et al. 4. In: Effects of erosion void on deteriorated metal culvert before and after repair with grouted slip liner, vol. 10; 2019, 04019031.
26. Qian H, Zong Z, Wu C, Li J, Gan L (2021) Numerical study on the behavior of utility tunnel subjected to ground surface explosion. Thin-Walled Structures 161:107422.
27. Raj Kumar R, Ilamparuthi K.: Experimental Study on the behavior of Buried flexible Plastic pipe. Electronic Journal of Geotechnical Engineering, 13:1-10 (2008).
28. Rakitin, B.; Ming, X. Centrifuge Modeling of Large Diameter Underground Pipes Subjected to Heavy Traffic Loads. Bull. South Ural. State Univ. Ser. Constr. Eng. Archit. 2016, 16, 31–46.
29. Saboya, F.; Tibana, S.; Reis, R.M.; Durand Farfan, A.; Rangel Melo, C.M.A. Centrifuge and Numerical Modeling of Moving Traffic Surface Loads on Pipelines Buried in Cohesionless Soil. Transp. Geotech. 2020, 23, 100340.
30. Schanz, T., P. A. Vermeer, and P. G. Bonnier. 1999. “The hardening soil model: Formulation and Verification.” In Beyond 2000 in computational geotechnics-10 years of PLAXIS. Rotterdam, Netherlands: A.A. Balkema.
31. Tafreshi SM and Khalaj O 2011 Analysis of repeated-load laboratory tests on buried plastic pipes in sand Soil Dynamics and Earthquake Engineering 31(1):1-15.
32. Tafreshi SM, et al. Buried pipes in rubber-soil backfilled trenches under cyclic loading. J Geotech Geoenviron Eng 2012;138(11):1346–56.

33. Talesnick M, Horany H, Dancygier AND, Karinski YS (2008) Measuring soil pressure on a buried model structure for the validation of quantitative frameworks. J Geotech Geoenviron Eng.
34. Tian, J.P.; Zhang, J.; Dong, F.F.; Du, G.F. Dynamic Response of Buried Pipeline Subject to Impact Loads Using Piezoceramic Transducers. Int. J. Press. Vessel. Pip. 2019, 177, 103984
35. Valsangkar AJ, Britto AM (1978) The validity of ring compression theory in the design of flexible buried pipes. Supplemental Rep. SR440, Transportation and Rock Research Laboratory, Crowthorne, UK.
36. Valsangkar AJ, Britto AM (1979) Centrifuge tests of flexible circular pipes subjected to surface loading. Supplemental Rep. SR530, Transportation and Rock Research Laboratory, Crowthorne, UK.
37. Zhang, Y., & Wong, R. C. K. (2023b). Effect of pipe installation and external load on buried steel pipe responses: Experimental and numerical investigations a Department of Civil Engineering, Schulich School of Engineering, University of Calgary, Calgary, AB T2N 1N4, Canada.
38. Zhou, M., Du, Y. J., Wang, F., & Liu, M. D. (2017). Performance of Buried HDPE Pipes. Part I: Peaking Deflection during Initial Backfilling Process. Geosynthetics International, 24(4), 383–395.